

Precision Limits of Low-Energy GNSS Receivers

Kenneth M. Pesyna, Jr., Robert W. Heath, Jr., and Todd E. Humphreys
The University of Texas at Austin

BIOGRAPHIES

Kenneth M. Pesyna Jr. is pursuing a Ph.D. in the Department of Electrical and Computer Engineering at The University of Texas at Austin, where he received his M.S. in 2011. He is a member of the UT Radionavigation Laboratory and the Wireless Networking and Communications Group. His research interests include indoor navigation and precise low-power mobile positioning.

Robert W. Heath Jr. is a professor in the Department of Electrical and Computer Engineering at The University of Texas at Austin where he holds the Cullen Trust for Higher Education Professorship in Engineering #6 and is Director of the Wireless Networking and Communications Group. He received his B.S. and M.S. in Electrical Engineering from the University of Virginia, and a Ph.D. in Electrical Engineering from Stanford University. His research interests include several aspects of wireless communication and signal processing: MIMO wireless communication, multiuser and multicell MIMO, adaptive video transmission, radionavigation, and millimeter wave communication techniques.

Todd E. Humphreys is an assistant professor in the Department of Aerospace Engineering and Engineering Mechanics at The University of Texas at Austin and Director of The University of Texas Radionavigation Laboratory. He received a B.S. and M.S. in Electrical and Computer Engineering from Utah State University and a Ph.D. in Aerospace Engineering from Cornell University. He specializes in applying optimal estimation and signal processing techniques to problems in radionavigation. His recent focus is on radionavigation robustness and security.

ABSTRACT

Limitations on position-time precision are analyzed in energy-constrained GNSS receivers. The goal of this work is to determine the combination of sampling rate, number of quantization bits, number of satellites tracked, and coherent integration time that maximizes the position-time precision under a fixed low-energy constraint. In this paper, only the measurement errors due to spectrally flat Gaussian thermal noise are considered. Analytical expressions relating the foregoing parameters to precision and energy consumption are developed. Based on these expressions, a constrained optimization problem is formulated. Optimal solutions indicate that under a tight energy constraint energy should be allocated toward increas-

ing the sampling rate at the expense of the other parameters. Moreover, the quantization resolution should be set above 1-bit only under an energy surplus. Interestingly, optimum settings under tight energy constraints approximately match those chosen by the designers of energy-efficient commercial GNSS receivers.

I. Introduction

Over the past decade, the performance parameters of consumer electronic devices such as disk capacity, processor speed, and wireless transfer data rate have experienced a Moore's-law-type exponential increase [1]. Battery energy density, on the other hand, has remained relatively stagnant [1]. For microchips, energy efficiency improves with decreasing feature size, making lithography technology the limiting factor. By contrast, for batteries, energy density is significantly limited by the size of the ions used to transfer charge [2]. Finding viable chemical processes with smaller ions has proven difficult. Consequently, power-conscious consumer-electronic engineers have been pressed to design more energy efficient devices. In the navigation industry, this means lower power GNSS chips as these have been shown to be a significant factor in the overall energy consumption of handheld electronic devices [3], [4].

There has been much prior work in the area of energy efficient GNSS receivers. Trends in state-of-the-art GNSS chipsets have led to power consumption levels on the order of 50 milliwatts for continuous tracking and 15 milliwatts for duty-cycled tracking [5]. Designers of these chipsets have focused on lowering their power consumption at the expense of positioning performance. A natural question to ask is as follows: what is the fundamental limit to the precision of a position-time fix under a specified energy constraint and what are the design parameters that achieve this limit? If this question could be answered, then device manufacturers could tune their devices to more nearly achieve it. This paper takes a first step by answering these questions under the simplifying assumption that all measurement errors are due to spectrally flat Gaussian thermal noise. Moreover, this paper focuses only on minimizing energy expended by the correlation and accumulation operations in the baseband processing, which is known to contribute significantly to a GNSS chip's overall energy budget.

This paper makes two main contributions. First, it identifies the analytical relationship between position-time precision, energy consumption, and four parameters of interest: sampling rate, quantization resolution, number of

satellites tracked, and coherent integration time. Second, it formulates a constrained optimization problem based on these analytical relationships. The solution to this problem reveals the combination of parameter values which maximizes the precision of a single-shot position-time fix that is limited to consume less than a specified amount of Joules.

Prior work has studied the effect that subsets of the parameters of interest have on the final position-time precision. For example, there has been work studying the effect that the number of quantization bits and the sampling rate have on a signal's carrier-to-noise ratio [6], [7]. Other work has derived lower bounds on code-tracking precision as a function of the carrier-to-noise ratio and the coherent integration time [8], [9]. Lastly, there has been work relating the code-tracking precision and the number of tracked satellites to the precision of the final position-time solution [10], [11]. The present study derives a succinct analytical relationship between the precision of the position-time solution and all four parameters of interest.

There has also been prior work studying the energy consumption of GNSS receivers. Researchers have shown that baseband processing accounts for over half of the energy consumed in modern GNSS receivers [12], [13]. This paper will focus solely on the energy consumed by the correlation and accumulation operations in the baseband processor. Although the full GNSS receiver energy consumption is not considered in this paper, as it leaves out, for example, the energy consumption of the radio-frequency (RF) front-end, valuable insights can still be gained from solving an optimization solution on behalf of the correlation and accumulation energy consumption alone.

The remainder of this paper is organized as follows. Section II derives the energy consumption of the baseband correlation and accumulation operations as a function of the four parameters of interest. Section III derives the receiver position-time precision as a function of the same four parameters. Section IV poses and solves the constrained optimization problem and studies parameter tradeoffs that are made to minimize the position-time error under fixed energy consumption. Section V discusses future work and conclusions are made in Section VI.

II. Receiver Energy Consumption

Of the energy consumed in baseband processing, a significant amount is assumed to be due to the bit-wise multiply and addition operations that occur during signal correlation and accumulation (CAA) [12], [14], that is, the dot product that occurs between the incoming intermediate-frequency signal and the locally-generated replica. This section will attempt to derive a simple, yet useful metric by which the total energy consumed by the CAA operations can be related to the sampling rate f_s , the number of quantization bits N_Q , the number of satellites tracked N_{SV} , and the code tracking integration time T_{coh} . Hereafter, these four quantities will be referred to as "param-

eters of interest."

A. Correlation and Accumulation Operation Count

During each CAA operation, a continuous batch of samples is multiplied sample-by-sample with a locally-generated signal replica and then summed together. The energy consumption of a CAA operation can be broken down into a series of binary multiplication and addition operations. In particular, a K -sample CAA consists of K N_Q -bit multiplication operations followed by $K-1$ $(N_Q + \log_2 K)$ -bit addition operations [15]. The $\log_2 K$ expression accounts for the maximum accumulator size that will be needed to store the final result.

A simple N_Q -bit carry-ripple binary adder consists of N_Q , 1-bit full-adders, and a simple N_Q -bit binary multiplier consists of a series of $N_Q - 1$, N_Q -bit carry-ripple binary adders. Accordingly, the entire CAA operation can be broken down into N_A , 1-bit full-adders where

$$\begin{aligned} N_A &= \underbrace{(K-1)(N_Q + \log_2 K)}_{\text{Accumulation Cost}} + \underbrace{K(N-1)(N)}_{\text{Multiplication Cost}} \\ &\approx K(N_Q + \log_2 K + N_Q^2 - N_Q) \text{ for large } K \\ &= K(N_Q^2 + \log_2 K). \end{aligned} \quad (1)$$

K is the total number samples in the CAA operation defined as

$$K = f_s T_{coh} \quad (2)$$

If operating a 1-bit full-adder costs E_A Joules, the total energy consumed by a CAA operation E_{CAA} can be approximated as

$$\begin{aligned} E_{CAA} &= E_A N_A \\ &= E_A f_s T_{coh} (N_Q^2 + \log_2 [f_s T_{coh}]). \end{aligned} \quad (3)$$

B. Approximation of Total Energy Consumption

Most GNSS receivers use an early-late code discriminator to estimate the code-phase of each GNSS signal and compute a pseudorange to each satellite. Receivers implementing this discriminator usually have two to three correlators: an early, a late, and, oftentimes, a prompt correlator. Each of these correlators computes complex correlation over a batch interval of length T_{coh} . A complex correlation consists of two separate correlations, an in-phase and quadrature-phase correlation. These correlations must be performed separately for each satellite tracked. Consequently, the total energy consumed by the CAA operations in a GNSS receiver E_{Total} can be written as a function of the number of CAAs to be performed and E_{CAA} :

$$\begin{aligned} E_{Total} &= \underbrace{3 \cdot 2 \cdot N_{SV}}_{\text{Number of CAAs}} E_{CAA} \\ &= 6 \cdot N_{SV} E_{CAA} \end{aligned} \quad (4)$$

where N_{SV} is the number of satellites being tracked.

III. Receiver Position-Time Error

The previous section approximated the total energy consumption due to signal correlation and accumulation in a GNSS receiver as a function of the four parameters of interest. This section will attempt to derive a lower bound on the position-time precision as a function of the same four parameters.

A. Relating Position-Time Error to Code-Tracking Error

This subsection will relate the overall position-time error to the channel-by-channel code-tracking error using what is known as the Geometric Dilution of Precision (GDOP). The RMS error of the combined position-time solution can be approximately modeled as a function of the GDOP and the code-tracking RMS error σ_u :

$$\sigma_{xyzt} = \sigma_u \cdot \text{GDOP}. \quad (5)$$

GDOP is defined as

$$\text{GDOP} = \sqrt{\text{Tr}(G^T G)^{-1}} \quad (6)$$

where G is the (M -by-4) geometry matrix constructed from the approximate unit direction vectors from the receiver to each tracked satellite. G and is defined as

$$G = \begin{bmatrix} \mathbf{1}^{(1)} & 1 \\ \mathbf{1}^{(2)} & 1 \\ \vdots & \vdots \\ \mathbf{1}^{(M)} & 1 \end{bmatrix}, \quad (7)$$

where

$$\mathbf{1}^{(k)} = \frac{(x^{(k)} - x_0, y^{(k)} - y_0, z^{(k)} - z_0)}{\|(x^{(k)} - x_0, y^{(k)} - y_0, z^{(k)} - z_0)\|} \quad (8)$$

is the (1-by-3) unit direction vector from the receiver to satellite k , and x^k , y^k , and z^k and x_0 , y_0 , and z_0 represent the respective positions of satellite k and the receiver in the Earth-centered, Earth-fixed reference frame. This definition of GDOP is dependent on a specific satellite geometry. For the optimization analysis presented hereafter, it is beneficial to obtain an estimate of GDOP that is not dependent on satellite geometry, but rather just a function of the number of satellites tracked. Along these lines, prior work has computed lower bounds on GDOP as a function of the number of satellites N_{SV} , assuming that these satellites are in an optimal geometry configuration [11], [16]. Reference [11] offers the following lower bound on GDOP:

$$\text{GDOP}_{\min} = \sqrt{\frac{10}{N_{SV}}}. \quad (9)$$

This bound assumes that the receiver can receive signals from any direction including negative elevation angles. Although a considerable simplification is made using this definition of GDOP, it will be beneficial to subsequent optimization analysis as it offers a smooth lower bound on GDOP as a function of N_{SV} .

B. Derivation of Code-Tracking Error

Equation (5) relates the RMS error of the position-time solution σ_{xyzt} to the RMS error of the pseudorange estimate σ_u as a function of GDOP. A lower bound on GDOP was presented in (9) as a function of N_{SV} , one of the four parameters of interest. This section will derive a practical lower-bound on σ_u as a function of the other three parameters f_s , T_{coh} , and N_Q , allowing us to derive σ_{xyzt} in terms of all four parameters.

B.1 Cramer-Rao Lower Bound

The Cramer-Rao lower-bound (CRLB) represents the absolute lower bound on the code-tracking error [17]. In [9], the CRLB for code-tracking error was derived for a batch of data of length T_{coh} :

$$\sigma_{u,\text{CRLB}}^2 = \frac{1}{2(2\pi)^2 T_{\text{coh}} \int_{-B_r/2}^{B_r/2} f^2 \frac{C_s G_s(f)}{G_w(f)} df} \quad (10)$$

$$= \frac{1}{2(2\pi)^2 T_{\text{coh}} \frac{C_s}{N_0} \int_{-B_r/2}^{B_r/2} f^2 G_s(f) df} \quad (11)$$

where

B_r is the captured signal bandwidth which is equal to the sampling rate for an ideal filter, i.e. $B_r = f_s$

C_s is the total received signal power

G_s is the GNSS signal power spectral density

G_w is the power spectral density of the noise plus interference

N_0 is the single-sided noise power spectral density

We are invoking the assumption, in (11), that our position-time precision is only affected by thermally flat Gaussian spectral noise.

For an infinitely long random square wave sequence, the power spectral density (PSD) can be derived as [18]:

$$G_s(f) = T_C \text{sinc}^2(\pi f T_C) \quad (12)$$

where T_C is the chip-length of the square wave, in seconds. Although the GPS L1 C/A code is not infinitely long, the PSD in (12) is a close approximation to the true PSD for this code. Assuming a receiver is tracking a GPS L1 C/A code, the CRLB for batch code-phase estimation can be simplified using (11) and (12) to

$$\sigma_{u,\text{CRLB}}^2 = \frac{1}{4T_{\text{coh}} \frac{1}{T_C} \frac{C_s}{N_0} \left(f_s - \frac{\sin(f_s \pi T_C)}{\pi T_C} \right)}. \quad (13)$$

B.2 Coherent Early-Late Discriminator

Although the CRLB offers a closed-form equation on the code-tracking error, it does so independent of a discriminator design [9]. Some estimators, like the batch least-squares estimator, have been shown to meet the CRLB, however, these require a large amount of computation, and consequently, energy, as code-phase estimates are found by computing cross correlations over a large number of time

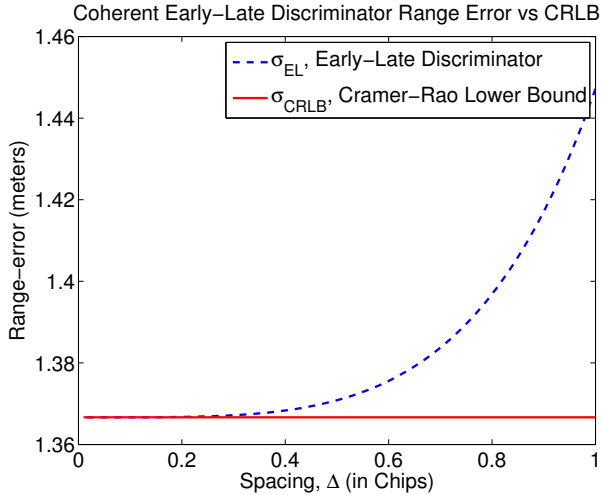


Fig. 1. Coherent early-late discriminator code-tracking error versus the Cramer-Rao lower bound as a function of the early-late tap spacing Δ . Here a GPS L1 C/A code is assumed with receiver parameters $T_{\text{coh}} = 2$ seconds, $\frac{C_s}{N_0} = 45$ dB-Hz, $f_s = 2$ MHz.

offsets or by taking the Fourier transform over all samples and solving a least squares problem in the frequency domain [19]. More preferable would be a lower-bound on a more-commonly used, lower-power discriminator. In particular, this paper will focus on the coherent early-late discriminator (CELD) as first introduced earlier in Sec. II-B during the discussion on energy consumption. A lower bound on the CELD code-tracking error would allow us to consider both the code-tracking error and the energy consumption in terms of the same discriminator mechanization, laying down the framework to pose the optimization problem in Sec. IV. The code-tracking error variance for a CELD has been derived as [9]:

$$\sigma_{u,\text{CELD}}^2 = \frac{\int_{-f_s/2}^{f_s/2} G_s(f) \sin^2(\pi f \Delta) df}{2(2\pi)^2 T_{\text{coh}} \frac{C_s}{N_0} \left(\int_{-f_s/2}^{f_s/2} f G_s(f) \sin(\pi f \Delta) df \right)^2} \quad (14)$$

where Δ is the early-late tap spacing, in seconds. In the limit as $\Delta \rightarrow 0$, (14) becomes equivalent to the CRLB, as illustrated in Fig. 1.

$$\lim_{\Delta \rightarrow 0} \sigma_{u,\text{CELD}}^2 = \sigma_{u,\text{CRLB}}^2 \quad (15)$$

Δ should be made as small as possible as it minimizes the estimated error variance. In application, however, the minimum Δ , in seconds, is limited by the sample spacing, that is

$$\min \Delta = \frac{1}{f_s}. \quad (16)$$

C. Effective Carrier-to-Noise Ratio

According to [6], the effective signal power received after complex correlation can be written as:

$$C_{\text{eff}} = |E[z_k]|^2 = (\bar{K} \cdot \bar{h}_{01})^2 \bar{R}_{\bar{s}s}[0] \cdot C = C/L_c \quad (17)$$

where L_c is the loss in power due to bandlimiting, sampling, and quantization

$$L_c = \frac{1}{[\bar{K} \cdot \bar{h}_{01} \cdot \bar{R}_{\bar{s}s}[0]]^2}. \quad (18)$$

with the following definitions

z_k is the complex correlation sum

\bar{K} is the quantizer gain coefficient defined in [6] as a function of the quantization resolution N_Q and the quantizer level thresholds.

\bar{h}_{01} is a quantizer coefficient defined in [6] as a function of the quantization resolution N_Q .

$\bar{R}_{\bar{s}s}[0]$ is the time-average of the discretized cross-correlation function between the filtered and desired signal. The parameter captures the signal power loss due to bandlimiting.

C the total received signal power impinging on the antenna, in watts

It is possible to show that:

$$\lim_{f_s \rightarrow \infty, N_Q \rightarrow \infty} C_{\text{eff}} = C. \quad (19)$$

The signal power loss due to f_s is already captured by the limits of integration in (14). However (14) does not account for the signal power losses due to N_Q . Consequently, it becomes important to replace the signal power term C_s in (14) by a term C'_s that accounts for this loss

$$C'_s = \frac{C_s}{L'_c} \quad (20)$$

where L'_c is the loss in signal power due to quantization only:

$$L'_c = \frac{1}{[\bar{K} \cdot \bar{h}_{01}]^2}. \quad (21)$$

Table I lists values of the signal power loss L'_c as a function N_Q , assuming optimal quantization threshold levels [6].

IV. Constrained Optimization Problem

This section sets up the constrained optimization problem using the analytical expressions defined for energy consumption and position-time error in Sections II and III. The problem is designed to minimize position-time error over the four parameters of interest subject to an energy constraint and is posed as follows:

$$\begin{aligned} & \underset{N_{\text{SV}}, N_Q, f_s, T_{\text{coh}}}{\text{minimize}} && \sigma_{\text{xyzt}}(N_{\text{SV}}, N_Q, f_s, T_{\text{coh}}) && (22) \\ & \text{subject to} && E_{\text{Total}} \leq \beta. \end{aligned}$$

TABLE I
SIGNAL POWER LOSS L'_c VERSUS QUANTIZATION RESOLUTION [6]

Quantization Resolution, N_Q (bits)	Signal Power Loss (dB)
1	1.96
2	0.55
3	0.17
4	0.05
5	0.02
6	0.01

The objective function is highly non-linear and has both real and integer objective variables. The sampling rate f_s and the integration time T_{coh} are real-valued while the number of tracked satellites N_{SV} and the quantization resolution N_Q are integer-valued. However, to make the solution tractable, these parameters will be assumed real-valued for subsequent analysis.

A. Tradeoffs Under Fixed Energy

Before solving the optimization problem posed in (22), it becomes useful to build intuition as to the significance of each parameter in terms of its benefit to the overall position-time precision per Joule consumed. A tradeoff analysis among the four parameters of interest assuming constant energy is produced as follows:

1. Fix receiver energy consumption according to (4) at $10^{11} \cdot E_A$ Joules and the carrier-to-noise ratio at $C/N_0 = 45$ dB-Hz.
2. Fix parameter values at $f_s = 2$ MHz, $T_{\text{coh}} = 1$ second, $N_{\text{SV}} = 8$ satellites, and $N_Q = 1$ bit when not being varied.
3. Solve for one parameter (the dependent parameter) as a function of a second parameter (the independent parameter) using Eqns. (1), (3), (4), and the fixed energy constraint.
4. For each value of the dependent and independent variable, solve for the position-time error using Eqns. (5), (14), (20), and the default values for the non-varying parameters.
5. Plot the position-time error as a function of the two varied parameters of interest.

Three tradeoff analyses are explored next, each involving two varied parameters of interest.

A.1 Integration Time versus Sampling Rate

This subsection analyzes the tradeoff between sampling rate f_s and integration time T_{coh} under fixed energy consumption. Fig. 2 plots the logarithm of the position-time RMS error σ_{xyzt} as a function of these two parameters. The dark trace, which is also projected onto the x-y axis for better visualization of the parameter values, illustrates parameter tradeoffs that can be made to maintain constant energy consumption. Naturally as f_s increases, T_{coh} decreases, because the added energy required to correlate

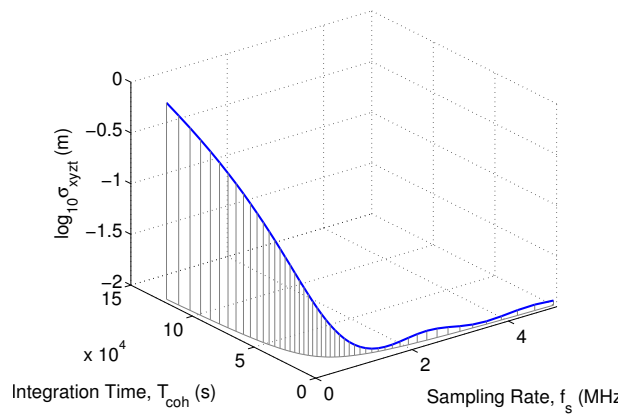


Fig. 2. Logarithm of the position-time error as a function of sampling rate f_s and integration time T_{coh} at fixed energy consumption.

at a faster sampling rate must be counteracted by a smaller integration time. From the figure, it is clear that energy should be allocated toward increasing the sampling rate past at least 1 MHz at the expense of a reduced integration interval, as the position-time error decreases rapidly up to that point. This is likely due to the large amount of signal power that is captured in the main lobe of the GPS signal power spectral density, which is approximately 2 MHz wide. After the sampling rate reaches 2 MHz, there is little change in the achievable position-time error as there is little remaining signal power to be gained from the signal side lobes. Any gains in positioning performance to be had from increasing f_s past this point will be offset by the necessary decrease in T_{coh} to maintain fixed energy consumption.

A.2 Number of Satellites versus Integration Time

This subsection analyzes the tradeoff between the number of tracked satellites N_{SV} and the integration time T_{coh} under fixed energy consumption. Fig. 3 plots the position-time RMS error σ_{xyzt} as a function of these two parameters. Once again, the dark trace illustrates parameter tradeoffs that can be made to maintain constant energy consumption. As N_{SV} increases, T_{coh} must be decreased to maintain constant energy consumption. Unlike in the first scenario, however, there is no benefit to any specific combination of the two parameters as the position-time error remains unchanged as one parameter is increased at the expense of decreasing the other. The intuition here is that the effect that T_{coh} has on the position-time precision is equivalent to that of N_{SV} for all combinations of the two under constant energy.

A.3 Quantization Resolution versus Sampling Rate

This subsection analyzes the tradeoff between quantization resolution N_Q and the sampling rate f_s under fixed energy consumption. Fig. 4 plots the position-time RMS error σ_{xyzt} as a function of these two parameters. Similar to the first scenario, increasing the sampling rate at the

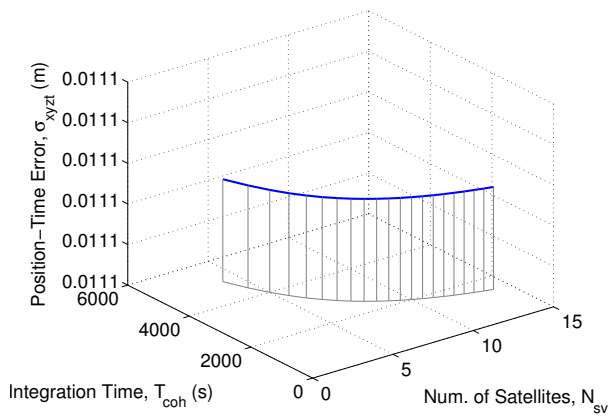


Fig. 3. Position-time error as a function of the number of tracked satellites N_{SV} and the integration time T_{coh} and at fixed energy consumption.

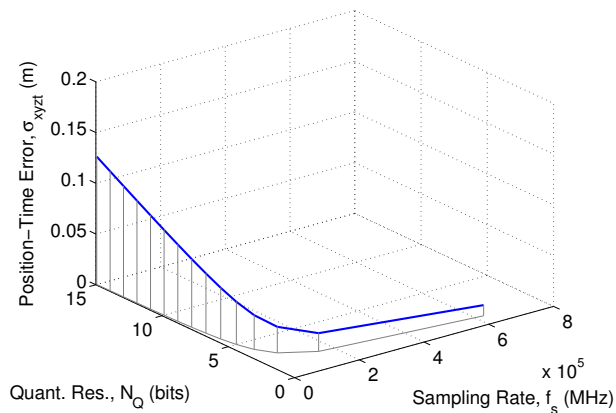


Fig. 4. Position-time error as a function of quantization resolution N_Q and sampling rate f_s at fixed energy consumption.

expense of decreasing the quantization resolution seems to yield the lowest position-time error. Unlike the first scenario, however, there is seemingly no plateau in the position-time error. The error continues to decrease as the sampling rate is increased to well in excess of 2 MHz. This insight suggests that to obtain the best positioning performance, the quantization resolution should be reduced to 1 bit and the remaining energy should be put toward maximizing the sampling rate.

B. Optimization Results

This subsection solves the constrained optimization problem posed in (22). As it is unwieldy to test all possible energy constraints and because some parameters must be bounded above or below, i.e. $4 \leq N_{SV} \leq 14$, an optimization solution will be performed around a set of nominal parameter bounds that model a typical low-power receiver setup. The solution strategy is as follows:

1. Fix $C/N_0 = 45$ dB-Hz and the energy constraint to $\beta = 1 \times 10^{13} \cdot E_A$ Joules.
2. Bound each objective variable to the values listed in Table II.

TABLE II
OBJECTIVE VARIABLE BOUNDS

	f_s (MHz)	T_{coh} (s)	N_{SV}	N_Q (bits)
Lower Bound	0.2	0.01	4	1
Upper Bound	3	10	12	10

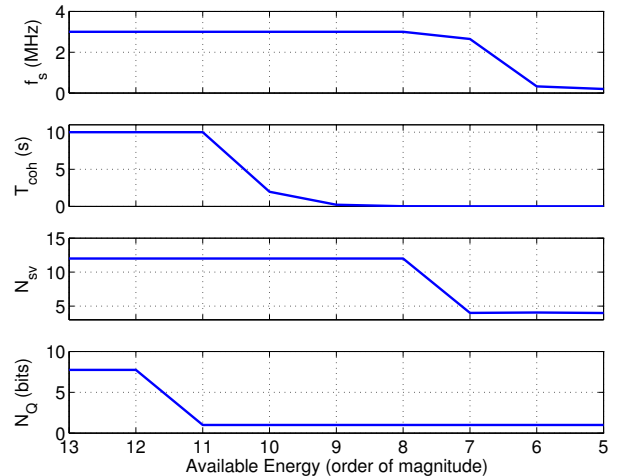


Fig. 5. Objective variable solutions to (22) as a function of a decreasing energy constraint. Objective variables are constrained by the bounds as listed in Table II.

3. Solve the constrained optimization problem of (22) using MATLAB's *fconmin* function [20], storing the objective variable values of the solution.
4. Decrease the energy constraint by one order of magnitude and repeat step 3 until the energy constraint reaches $\beta = 1 \times 10^5 \cdot E_A$ Joules.

As discussed previously, to make the optimization problem tractable, all objective variables will be assumed real-valued, even though they may not be in practice.

Figure 5 illustrates objective variable solutions to the optimization problem as a function of the decreasing available energy. It is apparent from the figure that with an abundance of energy, the solution to the optimization problem sets all objective variables to their upper bounds. However, as the available energy is decreased, it becomes clear that some of the objective variables are reduced prior to others. For example, the quantization resolution N_Q is the first objective variable to be reduced and is reduced almost immediately to its lower-bound-value of 1 bit. This result is reasonable because earlier derivations have shown that the baseband energy consumption increases as a function of N_Q^2 (see (3)), while the increase in captured signal power C'_s and thus the effect of N_Q on σ_{xyzt} levels off when $N_Q > 2$ bits (see Table I). The integration time T_{coh} and number of tracked satellites N_{SV} were the next two parameters to be reduced. The sampling rate was the last parameter to be reduced.

These results suggest an order of significance of the parameters of interest. By reducing some parameters while

keeping others maximized, the optimization problem determined that some parameters were “more valuable” per Joule in terms of minimizing σ_{xyzt} than others. The optimization problem performed as it was designed: strike the optimal balance between the impact each parameter has on minimizing σ_{xyzt} versus the impact it has on total energy consumption.

V. Future Work

Future work will relax the spectrally flat Gaussian thermal noise assumption and consider also the effect of multipath on the position-time precision. Multipath has been shown to be a dominant source of error in code-ranging systems [21], [22]. Multipath introduces a bias in the measured time delay that cannot be removed by increasing the integration time or narrowing the correlator taps [23]. Empirical tests performed in [23] suggest that the bias is often significant, but can be reduced by increasing f_s (see [23], Fig. 2). Future work will also consider a more complete energy consumption model where the energy consumed by the RF front-end will be analyzed as a function of the parameters of interest and incorporated into the optimization framework.

VI. Conclusions

Optimal tradeoffs between sampling rate, number of quantization bits, number of satellites tracked, and coherent integration time have been explored in maximizing the precision of a GNSS receiver’s position-time solution under a fixed energy constraint. Analytical expressions relating these tradeoffs to the position-time error and the baseband energy consumption have been developed and then used as objective and constraint functions in a constrained optimization problem. Results have revealed that quantization resolution is the least significant parameter in terms of its effect on the position-time error while the sampling rate is the most significant parameter. Accordingly, these results indicate that an energy-constrained GNSS receiver should allocate its energy resources toward increasing the sampling rate while decreasing the quantization resolution to 1-bit resolution. Finally, results have revealed that the optimal settings under the tight energy constraints explored in this paper approximately match those currently implemented in commercial GNSS receivers, revealing that device designers have naturally come to anticipate many of the same conclusions.

References

- [1] T. E. Starner, “Powerful change part 1: batteries and possible alternatives for the mobile market,” *Pervasive Computing, IEEE*, vol. 2, no. 4, pp. 86–88, 2003.
- [2] F. Schlachter, “No Moores law for batteries,” *Proceedings of the National Academy of Sciences*, vol. 110, no. 14, pp. 5273–5273, 2013.
- [3] A. Carroll and G. Heiser, “An analysis of power consumption in a smartphone,” in *Proceedings of the 2010 USENIX conference*, 2010, pp. 21–21.
- [4] Z. Zhuang, K.-H. Kim, and J. P. Singh, “Improving energy efficiency of location sensing on smartphones,” in *Proceedings of the 8th international conference on Mobile systems, applications, and services*. ACM, 2010, pp. 315–330.
- [5] *Datasheet: NEO-7 GPS/GNSS Module*, u-Blox, 2013.
- [6] C. Hegarty, “Analytical model for GNSS receiver implementation losses,” *NAVIGATION, Journal of the Institute of Navigation*, vol. 58, no. 1, p. 29, 2011.
- [7] J. Curran, D. Borio, and C. Murphy, “Front-end filtering and quantisation effects on GNSS signal processing,” in *1st International Conference on Wireless Communication, Vehicular Technology, Information Theory and Aerospace & Electronic Systems Technology*. IEEE, 2009, pp. 227–231.
- [8] C. Knapp and G. Carter, “The generalized correlation method for estimation of time delay,” *IEEE Transactions on Acoustics, Speech and Signal Processing*, vol. 24, no. 4, pp. 320–327, 1976.
- [9] J. Betz and K. Kolodziejcki, “Generalized theory of code tracking with an early-late discriminator part i: lower bound and coherent processing,” *IEEE Transactions on Aerospace and Electronic Systems*, vol. 45, no. 4, pp. 1538–1556, 2009.
- [10] P. Axelrad and R. G. Brown, *Global Positioning System: Theory and Applications*. Washington, D.C.: American Institute of Aeronautics and Astronautics, 1996, ch. 9: GPS Navigation Algorithms, pp. 409–434.
- [11] M. Zhang and J. Zhang, “A fast satellite selection algorithm: beyond four satellites,” *IEEE Journal of Selected Topics in Signal Processing*, vol. 3, no. 5, pp. 740–747, 2009.
- [12] B. Z. Tang, S. Longfield, S. A. Bhavé, and R. Manohar, “A low power asynchronous GPS baseband processor,” in *18th IEEE International Symposium on Asynchronous Circuits and Systems (ASYNC)*. IEEE, 2012, pp. 33–40.
- [13] C.-H. Wu, W.-C. Tsai, C.-G. Tan, C.-N. Chen, K.-I. Li, J.-L. Hsu, C.-L. Lo, H.-H. Chen, S.-Y. Su, K.-T. Chen *et al.*, “A GPS/Galileo soc with adaptive in-band blocker cancellation in 65nm cmos,” in *2011 IEEE International Solid-State Circuits Conference Digest of Technical Papers (ISSCC)*. IEEE, 2011, pp. 462–464.
- [14] J. Diaz, J. Garcia, and P. Roncagliolo, “An fpga implementation of a data-bit asynchronous GPS/GLONASS correlator,” in *2012 Argentine School of Micro-Nanoelectronics, Technology and Applications (EAMTA)*. IEEE, 2012, pp. 27–33.
- [15] W. Namgoong and T. H. Meng, “Minimizing power consumption in direct sequence spread spectrum correlators by resampling if samples-part i: performance analysis,” *IEEE Transactions on Circuits and Systems II: Analog and Digital Signal Processing*, vol. 48, no. 5, pp. 450–459, 2001.
- [16] M. Kihara and T. Okada, “A satellite selection method and accuracy for the global positioning system,” *NAVIGATION, Journal of the Institute of Navigation*, vol. 31, no. 1, pp. 8–20, 1984.
- [17] Y. Bar-Shalom, X. R. Li, and T. Kirubarajan, *Estimation with Applications to Tracking and Navigation*. New York: John Wiley and Sons, 2001.
- [18] P. Misra and P. Enge, *Global Positioning System: Signals, Measurements, and Performance*, revised second ed. Lincoln, Massachusetts: Ganga-Jumana Press, 2012.
- [19] K. M. Pesyna Jr. and T. E. Humphreys, “Whitepaper: Achieving the Cramer-Rao lower bound in GPS time-of-arrival estimation, a frequency domain weighted least-squares estimator approach,” 2013.
- [20] MATLAB Release 2013a. Natick, Massachusetts: The MathWorks Inc., 2013.
- [21] M. S. Braasch, “Isolation of GPS multipath and receiver tracking errors,” *NAVIGATION, Journal of the Institute of Navigation*, vol. 41, no. 4, pp. 415–434, 1994.
- [22] M. S. Braasch and M. F. DiBenedetto, “Spread-spectrum ranging multipath model validation,” *IEEE Transactions on Aerospace and Electronic Systems*, vol. 37, no. 1, pp. 298–304, 2001.
- [23] R. L. Fante and J. J. Vaccaro, “Evaluation and reduction of multipath-induced bias on GPS time-of-arrival,” *IEEE Transactions on Aerospace and Electronic Systems*, vol. 39, no. 3, pp. 911–920, 2003.